CEP55 3'-UTR promotes epithelial–mesenchymal transition and enhances tumorigenicity of bladder cancer cells by acting as a ceRNA regulating miR-497-5p

Chenglin Yang
General Hospital of Southern Theatre Command
Yue Yang
General Hospital of Southern Theatre Command
Wei Wang (wangweiccc@hotmail.com)
General Hospital of Southern Theatre Command
Wuer Zhou
Foshan Sanshui District People's Hospital
Xiaoming Zhang
General Hospital of Southern Theatre Command
Yuansong Xiao
General Hospital of Southern Theatre Command
Huifen Zhang
General Hospital of Southern Theatre Command

Research Article

Keywords: Competing endogenous RNA, CEP55, PTHLH, HMGA2, miR-497-5p, Bladder cancer

Posted Date: April 20th, 2022

DOI: https://doi.org/10.21203/rs.3.rs-1560146/v1

Abstract

Background: Centrosomal protein 55 (CEP55) is implicated in the tumorigenesis of bladder cancer (BC) but the detailed molecular mechanisms are unknown. We aim to develop a potential competing endogenous RNA (ceRNA) network related with CEP55 in BC.

Methods: We first extracted the expression profiles of RNAs from The Cancer Genome Atlas (TCGA) database and used bioinformatic analysis to establish ceRNAs in BC. Real-time quantity PCR (RT-qPCR) and immunohistochemical analysis were performed to measure CEP55 expression in different bladder cell lines and different grades of cancer. Bioinformatics analysis and luciferase assays were conducted to predict potential binding sites among miR-497-5p, CEP55, parathyroid hormone like hormone (PTHLH) and high mobility group A2 (HMGA2). Tumor xenograft model was used to show the effect of CEP55 3′-UTR on cisplatin therapy. Bioinformatics analysis, luciferase assays, and 5' rapid amplification of cDNA ends (5′RACE) were to explore the function of CEP55 3′-untranslated region (3′-UTR) on targeting miR-497-5p. Western blot and immunofluorescence assays were to detect the epithelial–mesenchymal transition (EMT) induction of CEP55 3′-UTR.

Results: CEP55 expression as well as the expression levels of the oncogenic proteins PTHLH and HMGA2 were upregulated in BC cells while miR-497-5p was downregulated. Low miR-497-5p expression and high CEP55 and HMGA2 expression levels were associated with more advanced tumor clinical stage and pathological grade. Overexpression of the CEP55 3′-UTR promoted the proliferation, migration, and invasion of the EJ cell line in vitro and accelerated EJ-derived tumor growth in nude mice, while inhibition of the CEP55 3′-UTR suppressed all of these oncogenic processes. In addition, CEP55 3′-UTR upregulation reduced the cisplatin sensitivity of BC cell lines and xenograft tumors. Bioinformatics analysis, luciferase assays, and 5′RACE suggested that the CEP55 3′-UTR functions as a ceRNA targeting miR-497-5p, leading to miR-497-5p downregulation and disinhibition of PTHLH and HMGA2 expression. Further, CEP55 downregulated miR-497-5p transcription by promoting NF-kB signaling. In turn, PTHLH and HMGA2 activated p38MAPK and ERK 1/2 pathways, and induced EMT of BC cells.

Conclusions: These results suggest that a ceRNA regulatory network involving CEP55 upregulates PTHLH and HMGA2 expression by suppressing endogenous miR-497-5p in bladder cancer.

Background

Bladder cancer (BC) is the most common urologic cancer worldwide and demonstrates both frequent local recurrence and distant metastasis. In most patients, BC is diagnosed at an advanced stage when successful therapeutic strategies are limited and mortality is high [1, 2]. A better understanding of the underlying molecular mechanisms of BC is crucial for developing novel therapeutics.

MicroRNAs (miRNAs) are 18–24 nucleotide single-stranded non-coding RNAs that negatively regulate target messenger RNA (mRNA) expression at the post-transcriptional level by binding to miRNA response elements (MREs) in the mRNA 3′-untranslated region (3′-UTR) [3, 4]. Dysregulation of miRNAs is

implicated in a growing number of diseases, including cancer [5]. RNA transcripts harboring 3'-UTR MREs shared with other mRNAs, called competitive endogenous RNAs (ceRNAs), can regulate mRNA expression levels by competing for the same pool of miRNAs [6, 7]. Theoretically, any RNA transcript that contains miRNA-binding sites is capable of sequestering miRNAs and acting as a ceRNA, so the previous pattern "miRNA→mRNA" now has been replaced by "ceRNA→miRNA→mRNA [8]. This competition between ceRNAs and mRNAs for miRNAs provides an additional level of genetic regulation that may also contribute to tumorigenesis and thus prove novel therapeutic targets against cancer.

Centrosomal protein 55 (CEP55), also designated FLJ10540, C10orf3, or URCC6, is a centrosome- and midbody-associated protein of ~ 55 kDa shown to be overexpressed in multiple human cancers [9], including colon cancer [10], epithelial ovarian carcinoma [11], gastric cancer [12], prostate cancer [13], and hepatocellular carcinoma [14], and is also implicated in bladder cancer (BC) tumorigenesis [15]. Despite the strong association with tumorigenesis, the precise functions of CEP55 in BC remained largely unexplored.

In this study, we show that the CEP55 3'-UTR can function as a ceRNA to promote metastasis, invasion, proliferation, and apoptosis resistance of bladder cancer cells by sponging miR-497-5p, thereby disinhibiting PTHLH and HMGA2 expression, which in turn activates p38MAPK and ERK 1/2 signaling pathways, leading to the induction of EMT. This study therefore defines several metastatic signaling pathways that could theoretically be targeted by novel therapeutics.

Methods

Data preparation and processing

Available mRNA sequencing (mRNA-seq) data and miRNA sequencing (miRNA-seq) data from 408 BLCA samples were gained from TCGA database(https://portal.gdc.cancer.gov/). All raw RNA-seq data (miRNAs and mRNAs) were normalized as fragments per kilobase of exon model per million mapped fragment reads. Transformation of miRNA sequences into human mature miRNA names was accomplished using the miRBase database (http://www.mirbase.org).

Screening of DEGs

When performing the differential expression analysis in $CEP55^{high}$ and $CEP55^{low}$ BLCA samples, we determined the differentially expressed genes (DEGs) with thresholds of $|logFC| > 1$ and $p < 0.05$. Volcano plots of the DERNAs (including DEmiRNAs and DEmRNAs) were visualized using R language (version 4.1.2).

Establishment of the ceRNA network in BC

The ceRNA network was constructed by the following steps: (1) ENCORI (StarBase, http://starbase.sysu.edu.cn/) was used to predict the potential miRNAs targeted by mRNA interaction pairs; (2) TargetScan (version 7.2, http://www.targetscan.org/) were used to forecast the target genes of

the DEmiRNAs and build the miRNA-mRNA interaction pairs; (3)The VennDiagram package in R software was utilized to compare the target genes with DEmRNAs, and the target genes that overlapped with DEmRNAs in this study were selected for the next analysis, thus building the ceRNA-miRNA-mRNA triple regulatory network.

The Cytoscape plug-in cytoHubba was performed to identify the hub ceRNA-miRNA-mRNA triple regulatory network. The generated networks were visualized by Cytoscape software (version 3.7.0, https://www.cytoscape.org/).

Cell culture

Three BC-derived cell lines (TCCSUP, T24, and 5637) and a normal bladder cell line (SV-HUC-1) were obtained from American Tissue Type Culture Collection (ATCC, Manassas, VA, USA), while the EJ bladder cancer cell line was obtained from Japanese Cancer Research Resources Bank (JCRB, Tokyo, Japan) and the BIU-87 bladder cancer cell line from China Center for Type Culture Collection (CCTCC, Wuhan, China). The TCCSUP line was cultured in the Dulbecco's modified Eagle's medium (DMEM, Gibco, Grand Island, NY) supplemented with 10% fetal bovine serum (FBS, Gibco) and 1% penicillin at 37°C under a humidified atmosphere containing 5% CO_2. The 5637, BIU-87, EJ, T24, and SV-HUC-1 lines were cultured in RPMI 1640 medium (Gibco) supplemented with 10% FBS and 1% penicillin at 37°C under a humidified atmosphere containing 5% CO_2.

Patients and tumor specimens

Bladder tumor samples and normal adjacent tissues were obtained from biopsy or surgical resection and analyzed in accordance with institutional guidelines on the use of human tissue. All patients provided informed written consent, and the study was approved by the Institute Research Ethics Committee, General Hospital of Southern Theatre Command, China. After biopsy or resection, all tissue samples were immediately frozen in liquid nitrogen and stored at -80°C for subsequent analysis. Samples were histologically confirmed as non-muscle-invasive bladder tumors (NMIBCs, n = 40), muscle-invasive bladder tumors (MIBCs, n = 30), and normal adjacent tissues (n = 70). Of these tumor samples, 35 were classified as low grade and 35 as high grade according to the TNM classification system and WHO criteria. In addition, a total of 59 fresh bladder tumor samples and normal adjacent tissues were used to detect the expression of CEP55 by qRT-PCR (Table 1, Fig. 1A,B).

Table 1
Correlation of the expression of CEP55 with clinicopathologic features.

Clinicopathologic features	n (%)	Relative expression of CEP55	*P*-value
Sex			0.573
Male	50(85)	5.52 ± 3.55	
Female	9(15)	4.81 ± 2.67	
Age (Year)			0.092
≤ 60	30(51)	4.68 ± 3.18	
60	29(49)	6.18 ± 3.55	
Tumor stage			0.001
CIS, Ta, T1(NMIBC)	38(64)	3.71 ± 2.18	
T2-T4(MIBC)	21(36)	8.49 ± 3.12	
Tumor grade			0.072
Low	35(59)	4.70 ± 2.80	
High	24(61)	6.46 ± 4.01	

Plasmid construction and transfection

To construct a CEP55 3'UTR overexpression plasmid, the human CEP55 mRNA 3'UTR cDNA sequence was amplified by polymerase chain reaction (PCR) using the forward primer 5'-CCGGAATTCCAAAATAAGTATTTGTTTTGATATTA-3' and reverse primer 5'-ATAAGAATGCGGCCGCTAAAACATTAAATAATTTTATTCT-3'. The amplification product was then digested with BamHI and Hind III, and cloned into the pcDNA3.1(+) plasmid (Invitrogen, Waltham, MA, USA). Human specific CEP55 siRNA, miR-497-5p mimic, miR-497-5p inhibitor, and normal control (NC) sequences were synthesized by RiboBio Biotechnology (RiboBio, Guangzhou, China) (Supplementary Table S1). All constructs were verified by DNA sequencing (Sangon Biotech, Shanghai, China).

For transfection, cells maintained as described at 5×10^5/well were harvested, reseeded in 6-well plates, and treated with 4 μg cDNA or 50 nM RNA plus Lipofectamine 2000 reagent (Invitrogen) according to the manufacturer's protocol. The efficiency of transfection was confirmed by quantitative real-time PCR (qRT-PCR) and western blot as described below.

RNA extraction and quantitative real-time PCR

Total RNA was extracted from patient bladder samples or cell lines using the RNA Universal Tissue Kit (Qiagen, Valencia, CA, USA) according to the manufacturer's instructions. A 2 μg total RNA sample was then reverse transcribed into cDNAs using ImProm-IITM Reverse Transcription System (Promega)

according to the manufacturer's manual. Quantitative RT-PCR for cDNA amplification and quantitation was performed using SYBR Green qPCR SuperMix (Invitrogen) according to the manufacturer's instructions on an ABI PRISM® 7500 Sequence Detection System (Applied Biosystems, Waltham, MA, USA). The thermocycle was 2 min at 50°C, 2 min at 95°C, and then 40 cycles of 95°C for 15 s and 60°C for 32 s. Primer sequences used for RT-PCR are listed in Supplementary Table S2. Expression levels of CEP55, HMGA2, and PTHLH were calculated using the $2^{-\Delta\Delta Ct}$ method with GAPDH as the internal control, while expression of miR-497-5p was measured with U6 snRNA as the internal control.

Wound healing assays

Cells were seeded into 6-well plates and transiently transfected as described. After 24 h, cells were allowed to grow to 90% confluence in complete medium. Cell monolayers were then wounded with a 200 µL sterile pipette tip and washed several times with phosphate buffered saline (PBS) to remove cell debris. The completed medium was then replaced with serum-free medium and incubation continued. Images of the scratch area (wound) were captured immediately and at 24 h post-scratch under an Olympus microscope (40×). Cells migrating into the wound surface and the average distance of migration were determined at designated time points (0 h and 24 h).

Transwell migration and invasion assays

Cells were transfected for 48 h with the indicated plasmid, harvested, and reseeded with serum-free media in the upper chambers of transwell culture dishes. The transwell inserts (8-µm pore size, Millipore, Burlington, MA, USA) were left untreated for migration assays or coated with Matrigel (BD Biosciences, Franklin Lakes, NJ) for invasion assays. Medium containing 10% FBS was added to the lower chambers as the chemoattractant and plates incubated at 37°C under a 5% CO_2 atmosphere for 48 h. The cells that had migrated or invaded through the membrane were fixed with methanol, stained with 0.1% crystal violet, and counted under an inverted microscope (Olympus, Tokyo, Japan).

Flow cytometry analysis of apoptosis

After transfection, cells were grown in serum-free conditions for 48 h. EJ cells stably expressing CEP55 3'-UTR and control cells transfected with empty plasmid were treated with 8 µmol/L cisplatin for 48 h, collected, washed with PBS, and labeled with 10 µL propidium iodide (PI) and 5 µL Annexin V/FITC (BD Biosciences) per 100 µL cell suspension (1×10^6 cells/mL). Cells were incubated in the dark for 15 min at room temperature and apoptosis assessed using a FACS Calibur system. The total number of apoptotic cells was determined by adding AnnexinV+/PI- and AnnexinV+/PI + cell fractions.

Stable cell lines

EJ cells stably overexpressing CEP55 3'UTR were obtained by transfection with pLVX-mCMV-ZsGreen-puro lentiviral vector containing full-length CEP55 3'UTR cDNA (produced according to the manufacturers' manual) using Lipofectamine 2000 (Invitrogen). Cells were selected by sustained incubation in 1 µg/mL puromycin for 2 weeks. The empty pLVX-mCMV-ZsGreen-puro vector was used to generate control cell lines.

Tumor xenograft model

EJ cells stably expressing CEP55 3′-UTR and control cells transfected with empty vector were collected and injected subcutaneously at 2×10^6 per 200 μL normal saline into 4-week-old female BALB/c nude mice obtained from the Laboratory Animal Center of Guangdong Medical College. All animal experiments were approved by the Institutional Animal Care and Use Committee of the General Hospital of Southern Theater Command. After 9 days, all mice exhibited palpable tumors. Mice were then randomly divided into two groups receiving either intraperitoneal cisplatin (4 mg/kg body weight in 0.5 mL saline) or equal-volume normal saline every 3 days. Tumor dimensions were measured weekly using a vernier caliper, and the volume calculated according to the formula

$$V = \frac{\pi L W^2}{6}$$

,

where L is length and W is width. All mice were sacrificed after 33 days and the final tumor weights were recorded.

Luciferase reporter assay

For miRNA target validation studies, HEK 293T cells were seeded in 24-well plates at 2×10^4 cells/well and transfected with hluct/hRluc luciferase reporter psiCHECK-2 vectors containing the wild-type (WT) or mutant (MUT) miR-497-5p binding sites of the CEP55 gene 3′UTR (psiCHECK-2/CEP55 3′UTR or psiCHECK-2/CEP55 MUT 3′UTR), HMGA2 gene 3′UTR (psiCHECK-2/HMGA2 3′UTR or psiCHECK-2/HMGA2 MUT 3′UTR), or PTHLH gene 3′UTR (psiCHECK-2 /PTHLH 3′UTR or psiCHECK-2 /PTHLH MUT 3′UTR) plus miR-497-5p mimic or control sequence. For the validation of ceRNA interaction, HEK 293T cells were co-transfected with psiCHECK-2 vectors containing the 3′UTR of HMGA2 or PTHLH and miR-497-5p, empty psiCHECK-2 vectors or vectors containing CEP55 3′UTR. Firefly luciferase activity relative to cell number was used to control for transfection efficiency. Forty-eight hours after transfection, luciferase activities were measured with the dual luciferase reporter assay system (Promega, Madison, WI, USA).

Western blot

Cells were lysed in RIPA buffer (50 mM Tris-Cl [pH 7.4], 150 mM NaCl, 1% TritonX-100, 1% sodium deoxycholate, 0.1% SDS, 1 mM EDTA) supplemented with protease and phosphatase inhibitor cocktail (Sigma, St. Louis, MO, USA). Protein concentrations were equalized across samples by measuring the total sample concentration using a BCA Protein Assay Kit (KEYGEN, China) and adding appropriate volumes of RIPA buffer. Total proteins were separated on 12% SDS-polyacrylamide gels and transferred onto PVDF membranes. Membranes were blocked with 5% skim milk for 1 h at room temperature and probed with the primary antibodies against the following proteins overnight at 4°C: CEP55 (1:100, sc-374051, Santa Cruz, Dallas TX, USA), PTHLH (1:200, sc-9680, Santa Cruz), HMGA2 (1:100, 8179, Cell

Signaling Technology, Danvers, MA, USA), TWIST (1:200, sc-15393, Santa Cruz,), E-cadherin (1:500, AF0131, Affbiotech, Cincinnati, OH, USA), Vimentin (1:500, AF7013, Affbiotech), Snail (1:500, AF6032, Affbiotech), ERK1/2 (1:200, sc-135900), p-ERK1/2 (Thr202/Tyr204) (1:200, Santa Cruz, sc-16982), MEK1/2 (1:200, sc-436, Santa Cruz),, p-MEK1/2 (Ser217/221) (1:1000, 9154P, Cell Signaling Technology), P38 (1:1000, 8690, Cell Signaling Technology), p-P38(Thy180/Tyr182) (1:200, sc-17852-R, Santa Cruz), and NF-κB p65 (Bioworld Technology, St. Louis Park, MN, USA). After primary antibody incubation, blots were washed three times with Tris-buffered saline containing 0.1% Triton X (TBST), incubated with appropriate secondary antibodies for 1 h at room temperature, and washed three times in TBST. Immunolabeling was visualized using Electro-Chemi-Luminescence (ECL) reagent.

Cell proliferation and colony forming assays

The MTT (3, 4, 5-dimethylthiazol-2, 5 biphenyl tetrazolium bromide, Invitrogen) cell viability assay was used to estimate proliferation rates in culture following the indicated treatments. After 48 h of transfection, cells were seeded on 96-well plates at 4×10^3 cells/well for 0, 24, 48, 72, and 96 h. Then, 20 μL MTT solution (5 mg/mL in Dulbecco's PBS) was added to each well and incubated for 4 h at 37°C. The culture medium was carefully removed and 200 μL of dimethyl sulfoxide added to dissolve the formazan generated by viable cells. Cell number was estimated by measuring the absorbance at 570 nm using a spectrophotometer. In other experiments, the MTT assay was conducted following treatment of 5×10^3 cells/well with cisplatin (0, 10, 20, 30, 40, and 50 μmol/L).

For colony-forming assays, cells were transfected for 48 h as described and seeded on 6-cm plates at 300 cells/well for 10 days at 37°C under a 5% CO_2. Then, the culture medium was carefully removed and remaining cells fixed with methanol and stained with 0.1% crystal violet. Culture wells were photographed under an inverted microscope and the number of colonies counted. Three independent experiments were performed with triplicate treatments.

Morphological assessment for endothelial–mesenchymal transition

Cells were seeded into 6-well plates, transiently transfected as described above, and incubated for 48 h, a time sufficient to allow EMT. Plates were washed with fresh medium to remove dead cells and examined at 100× magnification under a phase contrast microscope. Cells presenting mesenchymal characteristics, with a more fibroblast-like and long shuttle morphology, were considered as having undergone EMT.

Immunofluorescence staining

Cells were grown on glass chamber slides, fixed with 4% paraformaldehyde in PBS for 30 min, permeabilized in 0.1% Triton X-100 for 30 min, blocked with 3% bovine serum albumin in PBS for 1 h at room temperature, and then incubated sequentially with rabbit anti-human E-cadherin (AF0131, Affbiotech) and anti-vimentin antibody (AF7013, Affbiotech) overnight at 4°C and FITC-conjugated secondary antibody (Bioworld, Atlanta, Georgia, USA) for 1 h. Cells were washed with PBS between each step, then examined by laser scanning confocal microscopy.

In situ hybridization

For detection of miRNA expression in situ hybridization, 4-μm thick paraffin-embedded sections were mounted on tissue microarray (TMA) slides, incubated at 60°C for 1 h, deparaffinized in xylene, rehydrated with graded alcohol, washed three times with RNase-free PBS, digested with 8 mg/mL pepsin at 3°C for 10 min, washed, and then dehydrated in graded alcohol. Tissues were then hybridized with 50 nm locked nucleic acid (LNA)-modified DIG-labeled probes for miR-497-5p (Exiqon) at 40°C overnight. After stringency washes (5×, 1×, 0.2 × SSC), sections were incubated in blocking buffer for 30 min at room temperature and then overnight at 4°C in alkaline phosphatase-conjugated anti-DIG Fab fragment solution. Antibody signals were colorized with NBT and BCIP substrate and nuclei counterstained with Nuclear Fast Red.

Immunohistochemical staining

Immunohistochemistry was conducted on 5-mm formalin-fixed, paraffin-embedded tissue sections from BC patients (n = 70; General Hospital of Southern Theater Command, China) using antibodies against CEP55 (1:200, ab214302, Abcam, Cambridge, MA, USA) and HMGA2 (1:100, 8179, Cell Signaling Technology). Immunostaining was performed using the ChemMateTMDAKO EnVisionTM Detection Kit (DakoCytomation, Glostrup, Denmark). Subsequently, sections were counterstained with hematoxylin (Zymed Laboratories, South San Francisco, CA, USA) and mounted in nonaqueous mounting medium. The primary antibody was omitted for negative controls.

Immunohistochemical scoring

Immunohistochemical staining was assessed according to an immunoreactive score (IRS) that considered both staining intensity and the proportion of positive cells. Staining intensity was graded as 0 (no staining), 1 (weak), 2 (moderate), or 3 (strong), and the proportion of positive cells as 0 (negative), 1 (< 10%), 2 (10–50%), or 3 (> 50%). Intensity and positivity scores were multiplied to yield the IRS. An IRS ≥ 3 were defined as cytoplasmic expression positive and < 3 as negative.

Statistical analysis

All data were analyzed using SPSS (version 20.0). Results are presented as mean ± standard deviation (SD) of at least three independent experiments. Two group means were compared by two-sided Student's t-test and more than two group means by analysis of variance (ANOVA) with Bonferroni correction for pair-wise comparisons. $P < 0.05$ was considered significant for all tests.

Results

CEP55/miR-497-5p/HMGA2/PTHLH ceRNA network in BC

In the TCGA database, we found that CEP55 was overexpressed in BC, but down-expressed in normal tissues (Fig. 1A). Since CEP55 is abnormally overexpressed in tumor specimens, we then studied the

clinical significance of CEP55 expression in BC patients. Furthermore, we identified the differentially expressed miRNAs (DEmiRNAs) and differentially expressed mRNAs (DEmRNAs) in BC samples with $CEP55^{high}$ and $CEP55^{low}$ expression groups using TCGA database, with $P < 0.05$ and |log fold change [FC]| >1 as the miRNA and mRNA thresholds. In total, 31 DEmiRNAs (12 upregulated and 19 downregulated), and 1,454 DEmRNAs (825 upregulated and 629 downregulated) were sorted out from BC samples (Fig. 1B **and C**). To establish the ceRNA-miRNA-mRNA regulatory network in BC, we conducted a joint analysis in the $CEP55^{high}$ and $CEP55^{low}$ expression groups. We put the DEmiRNAs and DEmRNAs into the ENCORI database, and finally acquired 5 miRNAs (miR-23b, miR-200b, miR-200c, miR-429, miR-497) and 13 mRNAs (MAPK1, FOXK1, HMGA2, CEP55, PTHLH, NAV1, PPM1A, RAB22A, AFF4, PPTAR1, PRKCA, ARHGAP35, MKLN1) were involved in the ceRNA network. The Cytoscape plug-in cytoHubba was utilized to determine the hub triple regulatory network (Fig. 1D). Then, expression correlation analysis indicated there is a positive relationship among miR-497-5p, CEP55, HMGA2, and PTHLH (Fig. 1E). Together, we selected the CEP55/miR-497-5p/HMGA2/PTHLH axis in the ceRNA network as a potential prognostic model for the following step analysis.

CEP55 expression was upregulated in human BC tissues

We examined CEP55 gene expression in 59 paired bladder cancer samples and adjacent histologically normal tissues by qRT-PCR (normalized to GAPDH expression), and found that CEP55 was significantly upregulated in BC tissues compared to normal tissues (Fig. 2A). Similarly, immunohistochemical analysis (Fig. 2C) revealed significantly upregulated CEP55 protein expression in BC tissues compared to adjacent tissues according to immunoreactivity score (IRS). There was also a significant association between CEP55 overexpression and advanced tumor clinical stage (Fig. 2B) but not with patient sex, age, or tumor grade (Table 1). These results imply that CEP55 overexpression may be a useful biomarker for prognosis of BC.

We then investigated the expression level of miR-497-5p using situ hybridization and of CEP55 and HMGA2 proteins using immunohistochemistry in 70 bladder cancer samples, and found that low miR-497-5p expression and high levels of CEP55 and HMGA2 expression were associated with advanced tumor clinical stage as well as with higher pathology grade, but not with patient sex, age, or smoking status (Fig. 2C, **Supplementary Table S3-7**). These findings suggest the possibility that CEP55, HMGA2, or both are normally suppressed by miR-497-5p and that miR-497-5p downregulation allows for the uncontrolled upregulation (disinhibition) of one or both of these oncoproteins proteins.

CEP55, HMGA2, and PTHLH mRNAs were targeted by miR-497-5p

The microRNA-target interaction prediction programs TargetScan (http://www.targetscan.org) and miRanda (http://www.microrna.org/microrna/home.do) indicated that the 3’-UTRs of CEP55, HMGA2, and PTHLH mRNAs contain sites complementary to the seed region of miR-497-5p (Fig. 3A). Further, CEP55, HMGA2, and PTHLH were upregulated at both mRNA and protein levels in BC cell lines EJ, TCCSUP, 5637,

BIU-87, and T24 compared to the normal bladder cell line SV-HUC-1 (Fig. 3B-D, F). We also found that miR-497-5p was downregulated in all BC cell lines compared to SV-HUC-1 cells (Fig. 3E), consistent with negative regulation of CEP55, HMGA2, and PTHLH by miR-497-5p.

Further, miR-497-5p transfection markedly suppressed the relative luciferase activities of reporter plasmids containing the wild-type CEP55, HMGA2, or PTHLH 3’-UTR, but not the luciferase activities of reporters containing mutant CEP55, HMGA2, or PTHLH 3’-UTR (Fig. 3G, H, I), suggesting that all three 3’-UTRs bind miR-497-5p. To test whether CEP55, HMGA2, and PTHLH mRNAs are actually regulated by miR-497-5p, expression levels were examined in EJ cells co-transfected with miR-497-5p mimic or inhibitor. Expression levels of all three mRNAs were effectively increased by miR-497-5p inhibitor but suppressed by miR-497-5p mimic (Fig. 3J, K). Taken together, these results identify CEP55, HMGA2, and PTHLH mRNAs as potential targets of miR-497-5p.

CEP55 3’-UTR promoted metastasis, proliferation, and survival of EJ cells and these effects were mitigated by miR-497-5p

Cell migration and invasion capacities are critical for tumor metastasis. Based on our findings that CEP55 is overexpressed and miR-497-5p downregulated in BC as well the potential interaction between CEP55 mRNA and miR-497-5p, we predicted that CEP55 3’-UTR and miR-497-5p will alter BC cell viability, proliferation, migration, invasion, and (or) survival. Indeed, CEP55 3’-UTR overexpression or miR-497-5p inhibition promoted migration in the wound-healing assay (Fig. 4A,B,C), migration and invasion in transwell assays (Fig. 4D,E,F), and proliferation in the colony formation assay (Fig. 5A,B,C) and MTT assay (Fig. 5D,E,F), while suppressing apoptosis as evidenced by Annexin/PI staining and flow cytometry (Fig. 5G,H,I). Moreover, miR-497-5p overexpression or 3’-UTR CEP55 knockdown evoked the opposite responses. Further, co-expression of si-CEP55 blocked the effects of miR-497-5p inhibitor on cell migration, invasion, proliferation, and survival. These findings suggest that miR-497-5p normally serves to suppress tumorigenesis by downregulating CEP55 expression via 3’-UTR binding, while loss of CEP55 downregulation by miR-497-5p can promote tumorigenesis.

CEP55 3’-UTR reduced the cisplatin-sensitivity of EJ cells

To further investigate the effects of CEP55 3’-UTR on chemotherapy response, we established EJ cell lines stably overexpressing CEP55 3’-UTR using the pLVX-mCMV-ZsGreen-puro lentiviral vector. Overexpression of CEP55 3’-UTR was first confirmed by qRT-PCR (Fig. 6A). Annexin V/PI assays (Fig. 6B) and MTT assays (Fig. 6C) showed that CEP55 3’-UTR overexpression reduced BC cell apoptosis under treatment with cisplatin (8 μg/mL) and increased the cisplatin IC50 of BC cells compared to control EJ cells stably transfected with empty pLVX-mCMV-ZsGreen-puro lentiviral vector. Furthermore, stable overexpression of CEP55 3’-UTR increased the tumorigenic potential of EJ cells following subcutaneous injection in nude mice. Tumors were palpable 6 days after injection of EJ cells stably overexpressing CEP55 3’-UTR, whereas tumors were not palpable until 9 days after injection of cells stably expressing empty vector (control cells) (Fig. 6D-G). Tumors derived from EJ cells overexpressing CEP55 3’-UTR also

exhibited greater volume and weight than tumors derived from EJ cells transfected with empty vector after 33 days. Cisplatin treatment inhibited tumor growth in nude mice injected with control EJ cells but not tumors derived from EJ cells overexpressing CEP55 3’-UTR. These results are consistent with a tumorigenic function of CEP55 3’-UTR in vivo.

CEP55 3’-UTR upregulated HMGA2 and PTHLH expression by sponging miR-497-5p

We first examined if the CEP55 3’UTR influences the expression levels HMGA2, PTHLH, and miR-497-5p. We chose EJ cells, which expressed only moderate levels of endogenous CEP55 to construct the CEP55 3’-UTR overexpression cell line and TCCSUP cells, which highly expressed endogenous CEP55, to construct the CEP55 3’-UTR depletion cell line. The efficiency of CEP55 3-UTR regulation was first confirmed by qRT-PCR (Fig. 7A,B). Overexpression of CEP55 3’-UTR significantly reduced the expression of endogenous miR-497-5p (Fig. 7C) and significantly elevated the expression levels of HMGA2 and PTHLH (Fig. 7D,E). Conversely, CEP55 3’-UTR depletion significantly suppressed expression of HMGA2 and PTHLH, a response reversed by co-transfection of the miR-497-5p inhibitor (Fig. 7F). Collectively, these findings suggest a potential competitive endogenous RNA regulatory network involving miR-497-5p, CEP55, HMGA2, and PTHLH.

The nature of this interaction was then investigated directly using luciferase reporter plasmids containing CEP55, PTHLH, or HMGA2 3’-UTR fragments including the wild type miR-497-5p binding site. Overexpression of the CEP55 3’-UTR increased the luciferase activities of HMGA2 and PTHLH 3’-UTRs, suggesting that the CEP55 3’-UTR sequesters miR-497-5p due to higher binding affinity than HMGA2 and PTHLH 3’-UTRs (Fig. 7G, H). Therefore, the CEP55 3’-UTR acts as a ceRNA to upregulate the expression levels of HMGA2 and PTHLH mRNAs after transcription by competing for (inhibitory) miR-497-5p.

The pro-metastasis effect of the CEP55 3’UTR was associated with activation of NF-κB signaling and downregulation of miR-497-5p production

Cancer cells often acquire constitutively active NF-κB signaling to promote survival, metastasis, and proliferation [16]. Our results revealed CEP55 3’-UTR overexpression increased whereas CEP55 3’-UTR knockdown decreased NF-κB/p65 nuclear translocation (Fig. 8A–D). The microRNA-target interaction prediction program mribase (http://www.mirbase.org/) identified a promoter sequence of miR-497-5p upstream of the mature miRNAs sequence (Fig. 8E), and 5'RACE confirmed that the transcription initiation point (TSS) of miR-497-5p was located 3600 bp upstream of the pre-miR-497-5p sequence. We thus selected 2000 bp upstream of the TSS as the predicted range of transcription factor regulation and found two NF-κB binding sites using the transcription factor prediction website PROMO (http://alggen.lsi.upc.es/cgi-bin/promo_v3/promo/ promoinit.cgi?dirDB = TF_ 8.3) (Fig. 8F). Moreover, the binding sites of NF-κB in the upstream promoter region of miR-497-5p were confirmed by luciferase mutation assay and qRT-PCR (Fig. 8G). In summary, these results strongly suggest that the tumor-

promoting effect of the CEP55 3′-UTR is also mediated by NF-κB signaling and downregulation of miR-497-5p production.

The CEP55 3′-UTR induced EMT by activating p38MAPK and ERK 1/2 pathways

The morphology of EJ cells changed from ovoid to elongated following transfection with CEP55 3′-UTR overexpression vector or miR-497-5p inhibitor, which may enhance metastasis potential (Fig. 9A,B,C). The cell epithelial biomarker E-cadherin was also downregulated and the cell mesenchymal biomarkers vimentin, snail, and twist were upregulated in CEP55 3′-UTR-overexpressing EJ cells compared to empty vector-expressing EJ cells. Conversely, knockdown of the CEP55 3′-UTR in TCCSUP cells significantly increased the expression levels of mesenchymal markers (Fig. 9D,E). Moreover, immunofluorescence assays showed that the expression of E-cadherin was upregulated in EJ cells overexpressing the CEP55 3′-UTR (Fig. 9H), whereas vimentin expression was downregulated in CEP55 3′-UTR-transfected EJ cells compared to controls (Fig. 9I).

Finally, we investigated the effects of the CEP55 3′-UTR on activation of P38 MAPK and ERK 1/2 pathways, previously shown to induce EMT in BC cells overexpressing CEP55 3′-UTR (17–21). Indeed, CEP55 3′-UTR overexpression in EJ cells significantly increased P38, p-P38, MEK1/2, p-MEK1/2, ERK1/2, and p-ERK1/2 expression levels compared to control EJ cells, while CEP55 3′-UTR knockdown in TCCSUP cells reduced expression levels of these signaling proteins (Fig. 9F,G). In summary, these results indicate that CEP55 3′-UTR ultimately promotes EMT and tumorigenesis by activating P38MAPK and ERK 1/2 pathways.

Discussion

Through the Cancer Genome Atlas (TCGA) database, we found a potential ceRNA network of CEP55/miR-497-5p/HMGA2/PTHLH in BLCA by performing bioinformatics analysis. In our study, we observed that CEP55 expression was substantially upregulated in a large group of bladder cancer tissue samples (n = 59), and that elevated expression was associated with tumor clinical stage. Situ hybridization and immunohistochemical analysis showed that low miR-497-5p and high CEP55 and HMGA2 expression levels were associated with more advanced tumor clinical stage and pathological grade, but not with patient sex, age, or smoking status. Furthermore, the expression levels CEP55, PTHLH, and HMGA2 were upregulated, while the expression of miR-497-5p was downregulated in multiple BC cell lines. According to Pan-ceRNADB (http://www.biobigdata.com/pan-cernadb/) [22], CEP55, PTHLH, and HMGA2 may be co-regulated by common miRNAs. Further, the microRNA-target interaction databases TargetScan and miRanda revealed that the 3′-UTRs of CEP55, HMGA2, and PTHLH mRNAs contain complementary sites for the seed region of miR-497-5p. Individual miRNAs are known to target hundreds of mRNA transcripts, and each mRNA harbors multiple miRNA response elements (MREs) that can be regulated by several miRNAs. Moreover, different mRNA molecules can be targeted by same group of miRNAs. By competing for common miRNAs, protein-coding mRNA molecules can mutually regulate expression levels through

competition for shared miRNAs [23]. Based on these previous findings, we speculated that CEP55, PTHLH, and HMGA2 may also serve as ceRNAs by competing for miR-497-5p and that these molecular pathways regulate BC tumorigenesis and aggression.

Indeed, we found that the 3’-UTR of CEP55 functioned as a ceRNA able to enhance the expression levels of PTHLH and HMGA2 by sponging miR-497-5p in bladder cancer cells. The current prevailing view is that protein-coding genes must be translated into proteins to function, but recent studies have revealed that protein-coding mRNAs can achieve reciprocal regulation by competing for shared miRNAs, and that disruption of these complex networks can upset key physiological regulatory interactions and may support tumorigenesis [24, 25]. Kumar et al. reported that HMGA2 promoted lung cancer progression by acting as a ceRNA for the let-7 miRNA family [26]. In addition, high CEP55 expression has been found in human colon cancer [10], epithelial ovarian carcinoma [11], gastric cancer [12], prostate cancer [13], hepatocellular carcinoma [14], and BC [15]. Wang et al. found that CEP55 regulates the glucose metabolism, proliferation, and apoptosis of glioma cells via the Akt/mTOR signaling pathway [27]. The 3’-UTRs of protein-coding mRNAs frequently include miRNA binding sites (MREs) and thus may act as ceRNAs [28]. The current study showed that the promotion of EJ cell metastasis, proliferation, and survival by CEP55 3’-UTR overexpression could be mitigated by miR-497-5p overexpression, consistent with a putative competition (sponging) mechanism. Notable, overexpression of the CEP55 3’-UTR also reduced the sensitivity of EJ cells and EJ cell-derived tumors to cisplatin, underscoring the clinical importance of this CEP55 3’-UTR regulation pathway.

Epithelial-to-mesenchymal transition (EMT) is a complex process in which epithelial cells lose their characteristic features and acquire a mesenchymal-like phenotype. In tumors, this EMT increases the capacity of individual cells to disseminate to other parts of the body and colonize distant organs (metastasis) [29, 30]. Overexpression of the CEP55 3’-UTR or miR-497-5p inhibitor transfection changed EJ cell morphology from ovoid to oblong, which may have contributed to the greater migratory and invasive capacities of these cells, and also enhanced the expression levels of mesenchymal markers (vimentin, snail and twist) and reduce the level of the cell epithelial biomarker E-cadherin. Further, EMT promotion by CEP55 3’-UTR overexpression was counteracted by miR-497-5p. Our previous findings demonstrated that the CEP55 3’-UTR can function as a ceRNA to increase the expression levels of PTHLH and HMGA2 via disinhibition due to reduced miR-497-5p activity, and here we show that the tumor-promoting effect of CEP55 3’-UTR overexpression was mediated by sponging and by downregulation of miR-497-5p production in bladder cancer cells via NF-κB signaling. The parathyroid hormone-related protein (PTHrP), also designated as PTHLH, was originally identified as the factor responsible for malignant hypercalcemia and later found to be widely expressed in fetal and adult tissues. Today it is recognized that cytosolic PTHLH can use a bipartite multibasic nuclear localization signal to translocate to the nucleus and act through an intracrine pathway [31]. The high mobility group AT-hook 2 (Hmga2), a member of the HMG family of proteins, was first described in 1991 as a nuclear architectural protein that interacts with the minor groove of many AT-rich promoters and enhancers [32, 33]. A growing number of studies have revealed oncogenic functions for both PTHLH and HMGA2 in a variety of malignant tumors [30,34,35,36,37].

Recent studies have implicated aberrant activation of p38MAPK and ERK1/2 pathways in the proliferation, invasion, and metastasis of BC [17, 18, 19, 20, 21]. In renal tubuloepithelial cells, PTHLH induced EMT through activation of the ERK1/2 pathway while HMGA2 induced EMT through activation of the p38 MAPK pathway [38]. In addition, HMGA2 was reported to promote EMT and contribute to colon cancer progression by activating the p38MAPK pathway [39]. Based on these findings, we speculate that the CEP55 3′-UTR may induce the EMT of BC cells by reducing miR-497-5p-mediated suppression of PTHLH and HMGA2, thereby increasing expression of these two oncoproteins and enhancing p38 MAPK and ERK1/2 pathway activities. Consistent with this notion, we found that overexpression of the CEP55 3′-UTR increased P38, p-P38, MEK1/2, p-MEK1/2, ERK1/2, and p-ERK1/2 levels, and that these effects were mitigated by miR-497-5p. However, there is still no evidence that PTHLH and HMGA2 can directly activate P38MAPK and ERK 1/2 pathways in BC cells, an issue requiring additional study.

Abbreviations

BC, bladder cancer;

CEP55, centrosomal protein 55;

ceRNA, competing endogenous RNA;

DEGs, differentially expressed genes;

EMT, epithelial–mesenchymal transition;

HMGA2, high mobility group A2;

mRNA-seq, mRNA sequencing;

MIBCs, muscle-invasive bladder tumors;

PCR, polymerase chain reaction;

PTHLH, parathyroid hormone like hormone;

3′-UTR, 3′-untranslated region;

5′RACE, 5' rapid amplification of cDNA ends.

Declarations

Acknowledgements

We thank the patients and their families for the signed informed consent forms for clinical sample experiments. This study was supported by the Guangzhou Science and Technology Plan Project Basic

and Applied Basic Research Project (202002030030), and the Guangdong Province Basic and Applied Basic Research Fund Project (2020A1515010044).

Ethical approval and consent to participate:

The study involving humans was approved by the Research Ethics Committee of General Hospital of Southern Theater Command, No. 2019-034. The procedures used in this study adhere to the tenets of the Declaration of Helsinki. All informed consent was obtained from the subjects and guardians.

The study involving animals was approved by the Institutional Animal Care and Use Committee of the General Hospital of Southern Theater Command, No. 2019025b. The methods used in this study adhere to the tenets of the Declaration of Helsinki, and are in accordance with ARRIVE guidelines for the reporting of animal experiments.

Consent for publication: Not applicable

Availability of data and materials: The datasets generated and/or analysed during the current study are available in the TCGA-BLCA, NCBI and ensemble, [https://portal.gdc.cancer.gov/, https://www.ncbi.nlm.nih.gov/, and https://asia.ensembl.org/index.html].

Competing interest: The authors declare no potential conflicts of interest.

Funding: This study was supported by the Guangzhou Science and Technology Plan Project Basic and Applied Basic Research Project (202002030030), and the Guangdong Province Basic and Applied Basic Research Fund Project (2020A1515010044).

Author contributions

CLY, YY and WW designed the experimental protocols. CLY, YY, WW, WEZ performed the experiments. CLY, YY, WW, WEZ, XMZ, XXY, HFZ contributed to the writing and revision of the manuscript and analyzed the data. CLY, WW, XMZ, XXY, HFZ contributed to the material support of the study. All authors read and approved the final manuscript.

References

1. Zhao F, Lin T, He W, Han J, Zhu D, Hu K, et al. Knockdown of a novel lincRNA AATBC suppresses proliferation and induces apoptosis in bladder cancer. Oncotarget. 2015;6(2):1064–78. doi: 10.18632/oncotarget.2833.
2. Zhuang J, Lu Q, Shen B, Huang X, Shen L, Zheng X, et al. TGFbeta1 secreted by cancer-associated fibroblasts induces epithelial-mesenchymal transition of bladder cancer cells through lncRNA-ZEB2NAT. Scientific Reports. 2015;5:11924. doi: 10.1038/srep11924.

3. Ruvkun G. Clarifications on miRNA and cancer. Science (New York, NY). 2006;311(5757):36–7. doi: 10.1126/science.311.5757.36d.
4. Poliseno L, Salmena L, Zhang J, Carver B, Haveman WJ, Pandolfi PP. A coding-independent function of gene and pseudogene mRNAs regulates tumour biology. Nature. 2010;465(7301):1033–8. doi: 10.1038/nature09144.
5. Tay Y, Kats L, Salmena L, Weiss D, Tan SM, Ala U, et al. Coding-independent regulation of the tumor suppressor PTEN by competing endogenous mRNAs. Cell. 2011;147(2):344–57. doi: 10.1016/j.cell.2011.09.029.
6. Salmena L, Poliseno L, Tay Y, Kats L, Pandolfi PP. A ceRNA hypothesis: the Rosetta Stone of a hidden RNA language? Cell. 2011;146(3):353–8. doi: 10.1016/j.cell.2011.07.014. Epub 2011 Jul 28.
7. Jeffery J, Sinha D, Srihari S, Kalimutho M, Khanna KK. Beyond cytokinesis: the emerging roles of CEP55 in tumorigenesis. Oncogene. 2016;35(6):683–90. doi: 10.1038/onc.2015.128.
8. Sakai M, Shimokawa T, Kobayashi T, Matsushima S, Yamada Y, Nakamura Y, et al. Elevated expression of C10orf3 (chromosome 10 open reading frame 3) is involved in the growth of human colon tumor. Oncogene. 2006;25(3):480–6. doi: 10.1038/sj.onc.1209051
9. Zhang W, Niu C, He W, Hou T, Sun X, Xu L, et al. Upregulation of centrosomal protein 55 is associated with unfavorable prognosis and tumor invasion in epithelial ovarian carcinoma. Tumour biology. 2016;37(5):6239–54. doi: 10.1007/s13277-015-4419-6.
10. Tao J, Zhi X, Tian Y, Li Z, Zhu Y, Wang W, et al. CEP55 contributes to human gastric carcinoma by regulating cell proliferation. Tumour biology: the journal of the International Society for Oncodevelopmental Biology and Medicine. 2014;35(5):4389–99. doi: 10.1007/s13277-013-1578-1.
11. Shiraishi T, Terada N, Zeng Y, Suyama T, Luo J, Trock B, et al. Cancer/Testis Antigens as potential predictors of biochemical recurrence of prostate cancer following radical prostatectomy. Journal of Translational Medicine. 2011;9:153. doi: 10.1186/1479-5876-9-153.
12. Chen CH, Lu PJ, Chen YC, Fu SL, Wu KJ, Tsou AP, et al. FLJ10540-elicited cell transformation is through the activation of PI3-kinase/AKT pathway. Oncogene. 2007;26(29):4272–83. doi: 10.1038/sj.onc.1210207.
13. Singh PK, Srivastava AK, Rath SK, Dalela D, Goel MM, Bhatt ML. Expression and clinical significance of Centrosomal protein 55 (CEP55) in human urinary bladder transitional cell carcinoma. Immunobiology. 2015;220(1):103–8. doi: 10.1016/j.imbio.2014.08.014.
14. DiDonato JA, Mercurio F, Karin M. NF-κB and the link between inflammation and cancer. Immunol Rev. 2012;246(1):379–400. doi: 10.1111/j.1600-065X.2012.01099.x.
15. Motoyama K, Inoue H, Nakamura Y, Uetake H, Sugihara K, Mori M. Clinical significance of high mobility group A2 in human gastric cancer and its relationship to let-7 microRNA family. Clinical Cancer Research. 2008;14(8):2334–40. doi: 10.1158/1078-0432.CCR-07-4667.
16. He H, Chang R, Zhang T, Yang C, Kong Z. ATM mediates DAB2IP-deficient bladder cancer cell resistance to ionizing radiation through the p38MAPK and NF-kappaB signaling pathway. Molecular Medicine Reports. 2017;16(2):1216–1222. doi: 10.3892/mmr.2017.6689.

17. Slusser-Nore A, Garrett SH, Zhou XD, Sens DA, Sens MA, Somji S. The expression of keratin 6 is regulated by the activation of the ERK1/2 pathway in arsenite transformed human urothelial cells. Toxicology and Applied Pharmacology. 2017;331:41–53. doi: 10.1016/j.taap.2017.05.007.
18. Lv D, Wu H, Xing R, Shu F, Lei B, Lei C, et al. HnRNP-L mediates bladder cancer progression by inhibiting apoptotic signaling and enhancing MAPK signaling pathways. Oncotarget. 2017;8(8):13586–13599. doi: 10.18632/oncotarget.14600.
19. Sun X, Deng Q, Liang Z, Liu Z, Geng H, Zhao L, et al. Cigarette smoke extract induces epithelial-mesenchymal transition of human bladder cancer T24 cells through activation of ERK1/2 pathway. Biomedicine & Pharmacotherapy = Biomedecine & Pharmacotherapie. 2017;86:457–465. doi: 10.1016/j.biopha.2016.12.022.
20. Calabro F, Lorusso V, Rosati G, Manzione L, Frassineti L, Sava T, et al. Gemcitabine and paclitaxel every 2 weeks in patients with previously untreated urothelial carcinoma. Cancer. 2009;115(12):2652–9. doi: 10.1002/cncr.24313.
21. Xu J, Li Y, Lu J, Pan T, Ding N, Wang Z, et al. The mRNA related ceRNA-ceRNA landscape and significance across 20 major cancer types. Nucleic Acids Research. 2015;43(17):8169–82. doi: 10.1093/nar/gkv853.
22. Ergun S, Oztuzcu S. Oncocers: ceRNA-mediated cross-talk by sponging miRNAs in oncogenic pathways. Tumour Biology. 2015 May;36(5):3129–36. doi: 10.1007/s13277-015-3346-x.
23. Chiu HS, Martinez MR, Bansal M, Subramanian A, Golub TR, Yang X, et al. High-throughput validation of ceRNA regulatory networks. BMC Genomics. 2017;18(1):418. doi: 10.1186/s12864-017-3790-7.
24. Kumar MS, Armenteros-Monterroso E, East P, Chakravorty P, Matthews N, Winslow MM, et al. HMGA2 functions as a competing endogenous RNA to promote lung cancer progression. Nature. 2014;505(7482):212–7. doi: 10.1038/nature12785.
25. Wang G, Liu M, Wang H, Yu S, Jiang Z, Sun J, et al. Centrosomal protein of 55 regulates glucose metabolism, proliferation and apoptosis of glioma cells via the Akt/mTOR signaling pathway. Journal of Cancer. 2016;7(11):1431-40. doi: 10.7150/jca.15497. eCollection 2016.
26. Zheng T, Chou J, Zhang F, Liu Y, Ni H, Li X, et al. CXCR4 3'UTR functions as a ceRNA in promoting metastasis, proliferation and survival of MCF-7 cells by regulating miR-146a activity. European Journal of Cell Biology. 2015;94(10):458–69. doi: 10.1016/j.ejcb.2015.05.010.
27. Lamouille S, Xu J, Derynck R. Molecular mechanisms of epithelial-mesenchymal transition. Nature Reviews Molecular Cell Biology. 2014;15(3):178–96. doi: 10.1038/nrm3758.
28. Nieto MA. Epithelial plasticity: a common theme in embryonic and cancer cells. Science (New York, NY). 2013;342(6159):1234850. doi: 10.1126/science.1234850.
29. Wang X, Liu X, Li AY, Chen L, Lai L, Lin HH, et al. Overexpression of HMGA2 promotes metastasis and impacts survival of colorectal cancers. Clinical Cancer Research. 2011;17(8):2570–80. doi: 10.1158/1078-0432.CCR-10-2542.
30. Morishita A, Zaidi MR, Mitoro A, Sankarasharma D, Szabolcs M, Okada Y, et al. HMGA2 is a driver of tumor metastasis. Cancer Research. 2013;73(14):4289–99. doi: 10.1158/0008-5472.CAN-12-3848.

31. Wu J, Liu Z, Shao C, Gong Y, Hernando E, Lee P, et al. HMGA2 overexpression-induced ovarian surface epithelial transformation is mediated through regulation of EMT genes. Cancer Research. 2011;71(2):349–59. doi: 10.1158/0008-5472.CAN-10-2550.
32. Cao R, Meng Z, Liu T, Wang G, Qian G, Cao T, et al. Decreased TRPM7 inhibits activities and induces apoptosis of bladder cancer cells via ERK1/2 pathway. Oncotarget. 2016;7(45):72941–72960. doi: 10.18632/oncotarget.12146.
33. Ongkeko WM, Burton D, Kiang A, Abhold E, Kuo SZ, Rahimy E, et al. Parathyroid hormone related-protein promotes epithelial-to-mesenchymal transition in prostate cancer. PloS One. 2014;9(1):e85803. doi: 10.1371/journal.pone.0085803.
34. Li Y, Zhao Z, Xu C, Zhou Z, Zhu Z, You T. HMGA2 induces transcription factor Slug expression to promote epithelial-to-mesenchymal transition and contributes to colon cancer progression. Cancer Letters. 2014;355(1):130–40. doi: 10.1016/j.canlet.2014.09.007.

Figures

Figure 1

CEP55/miR-497-5p/HMGA2/PTHLH ceRNA network in bladder cancer (BC). (A) Expression distribution of CEP55 in pan-cancer tissues. (B-C) 31 DEmiRNAs (|log2fold change| > 1 and adjusted p value < 0.05) and 1454 DEmRNAs (|log2fold change| > 1 and adjusted p value < 0.05). Red represents upregulated genes and blue indicates downregulated genes. (D) Eighteen hub genes in this network with a score of >2. (E) Correlations of relative RNAs in BC.

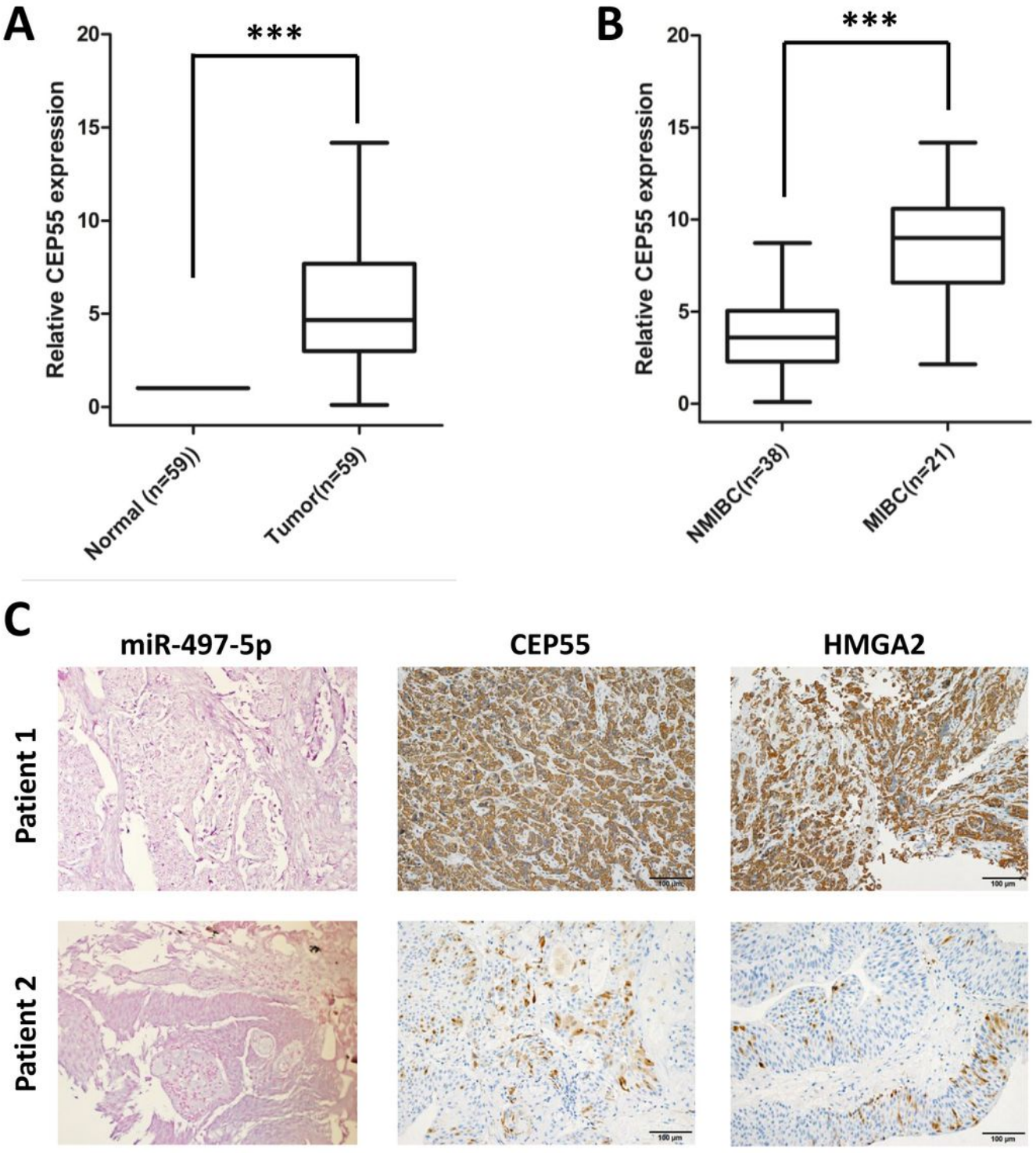

Figure 2

Elevated CEP55 expression in BC tissue and associations with higher clinical stage and expression levels of miR-497-5p and HMGA2. (A) Relative expression of CEP55 mRNA in BC tissues (n = 59) compared to adjacent non-tumor normal control (NC) tissues (n = 59) as examined by qRT-PCR (normalized to GAPDH expression). Data are presented as fold-change relative to normal tissues. (B) Relative expression levels of CEP55 in non-muscle invasive BC (n =38) and muscle-invasive BC (n = 21) as determined by qRT-PCR.

Expression was significantly higher in the more advanced muscle-invasive BC. (C) Expression levels of miR-497-5p, CEP55, and HMGA2 in representative BC patient samples as examined by in situ hybridization (miR-497-5p) or immunohistochemistry (CEP55 and HMGA2). Patient 1 exhibited low-level expression of miR-497-5p and high-level expression of both CEP55 and HMGA2, whereas patient 2 exhibited high-level expression of miR-497-5p and low-level expression of both CEP55 and HMGA2. Data in A and B presented as mean ± SD, n = 3 replicates per sample, $*P < 0.05$, $**P < 0.01$, $***P < 0.001$ vs. NC group.

Figure 3

Targeting of CEP55, PTHLH, and HMGA2 3'-UTRs by miR-497-5p. (A) Prediction of consequential pairing regions between miR-497-5p and the 3'UTRs of CEP55, PTHLH, and HMGA2 using Targetscan and miRanda. (B-E) Expression levels of miR-497-5p, CEP55 mRNA, PTHLH mRNA, and HMGA2 mRNA in different bladder cancer cell lines (5637, BIU-87, EJ, T24, TCCSUP), a normal human bladder epithelial cell line (SV-HUC-1), and normal bladder tissue as measured by qRT-PCR. (F) Expression levels of CEP55, PTHLH, and HMGA2 proteins in bladder cancer cells (5637, BIU-87, EJ, T24, TCCSUP), a normal human bladder epithelial cell line (SV-HUC-1), and normal bladder tissue as measured by western blot. (G-I) Hluct/hRluc luciferase reporter assays of 293T cells transfected with psiCHECK-2 vectors containing the wild type or a mutated miR-497-5p binding site from the 3'UTR of CEP55 (G), PTHLH (H), or HMGA2 (I) plus miR-497-5p-mimic or miR-NC. Luciferase activities were measured 48 h after transfection. (J and K) Effects of miR-497-5p overexpression on CEP55, PTHLH and HMGA2 mRNA and protein expression levels. EJ cells were transfected with miR-497-5p mimic, miR-497-5p inhibitor, or miR-NC. Gene expression levels were measured by qRT-PCR 48 h after transfection.

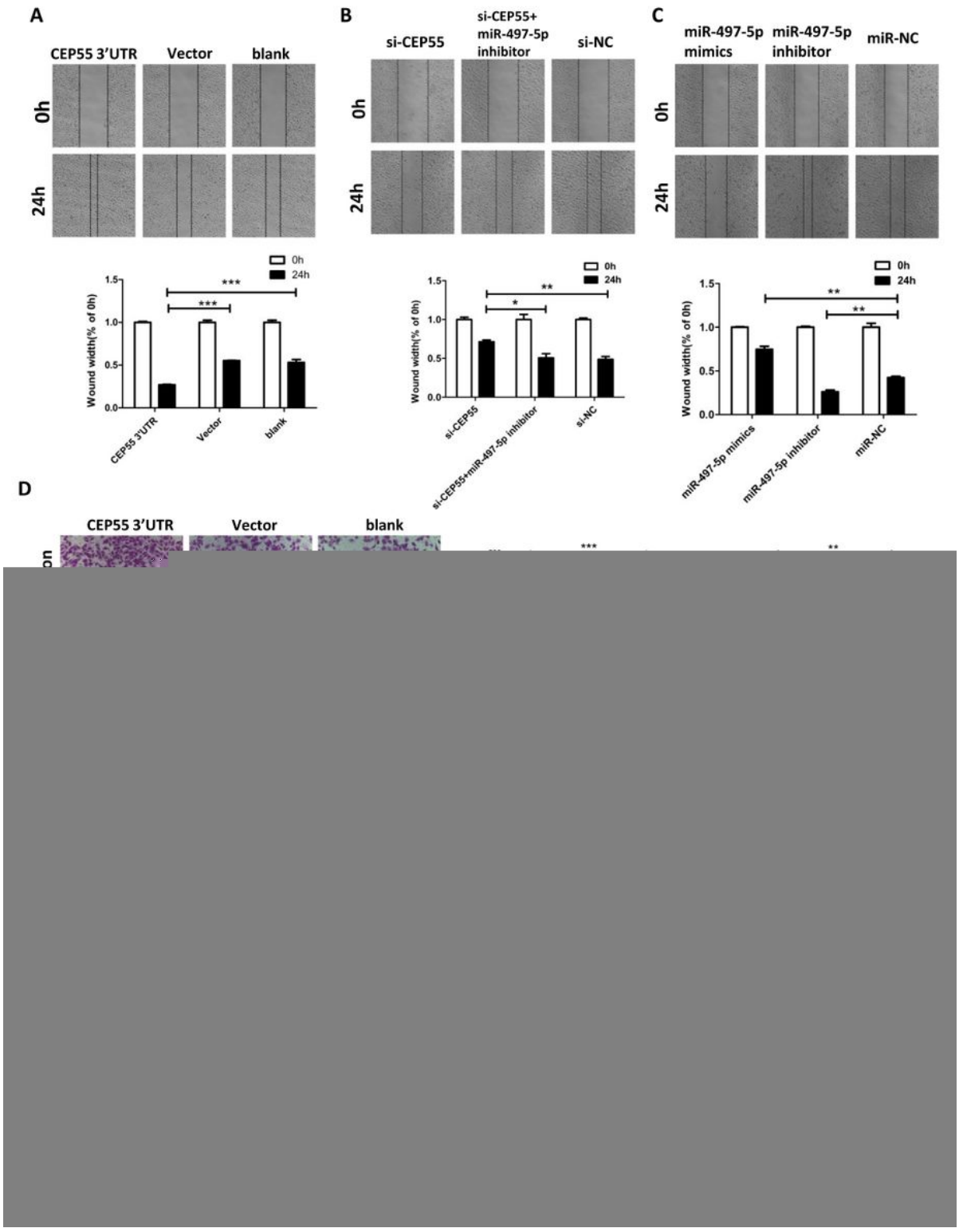

Figure 4

Overexpression of the CEP55 3'UTR increased migration and invasive capacities of EJ cells and these changes were reversed by miR-497-5p. (A-C) Effects of CEP55 3'UTR overexpression with and without miR-497-5p co-transfection on EJ cell migration as measured by the wound healing assay. (D-F) Effects of CEP55-3'UTR overexpression with and without miR-497-5p co-transfection on EJ cell migration and invasion as measured by transwell assays.

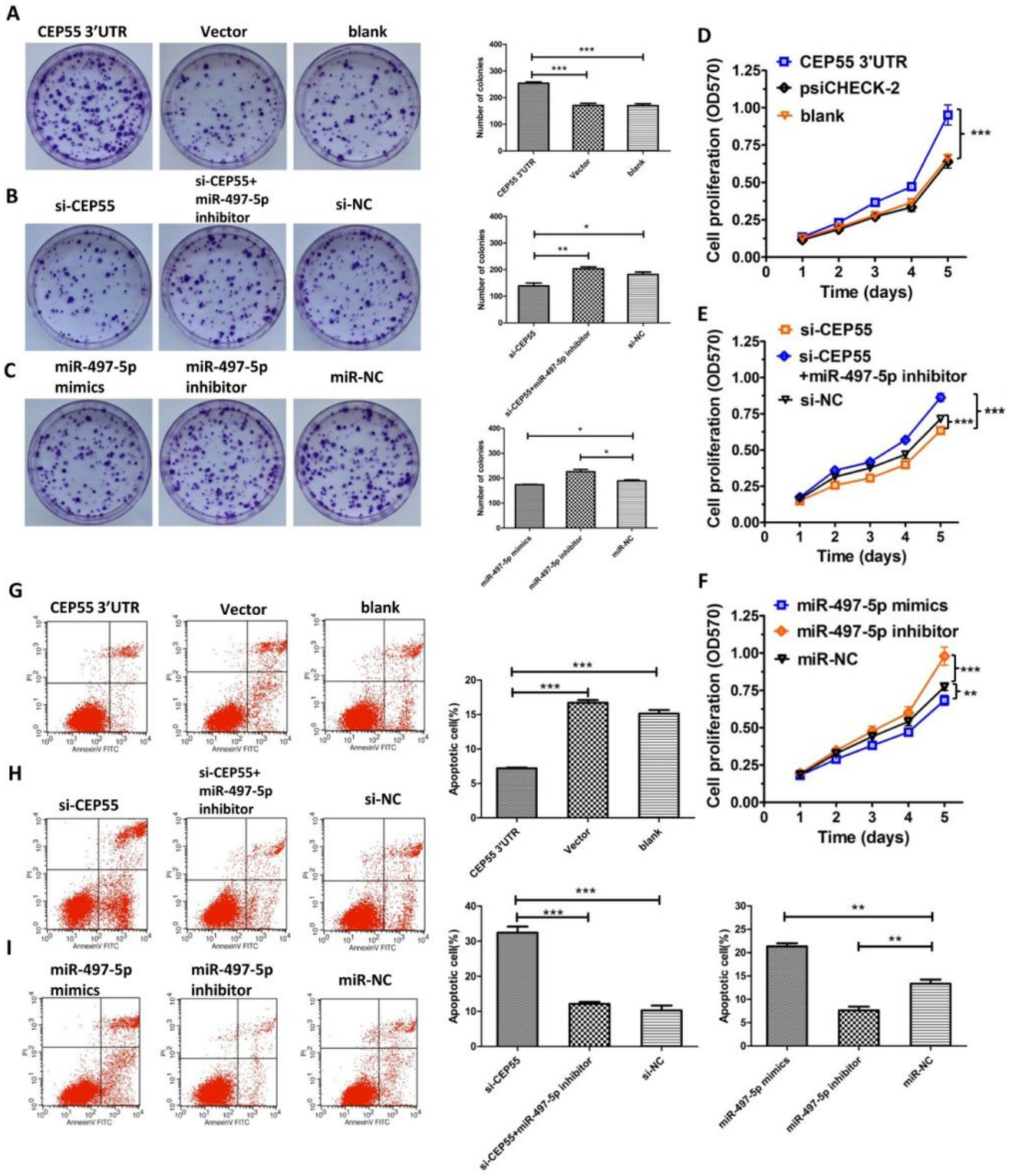

Figure 5

CEP55-3'-UTR promoted proliferation and inhibited apoptosis of EJ cells, effects reversed by miR-497-5p. (A-F) Effects of CEP55-3'UTR overexpression with and without miR-497-5p co-transfection on EJ cell proliferation as measured by MTT viability assay and colony-forming assay. (G-I) Effects of CEP55-3'UTR overexpression with or without miR-497-5p co-transfection on the apoptosis rate of EJ cells as assessed

by Propidium Iodide (PI)/Annexin V staining and flow cytometry. Apoptotic cells are Annexin V-FITC-positive/PI-negative or Annexin V-FITC-positive/PI-positive.

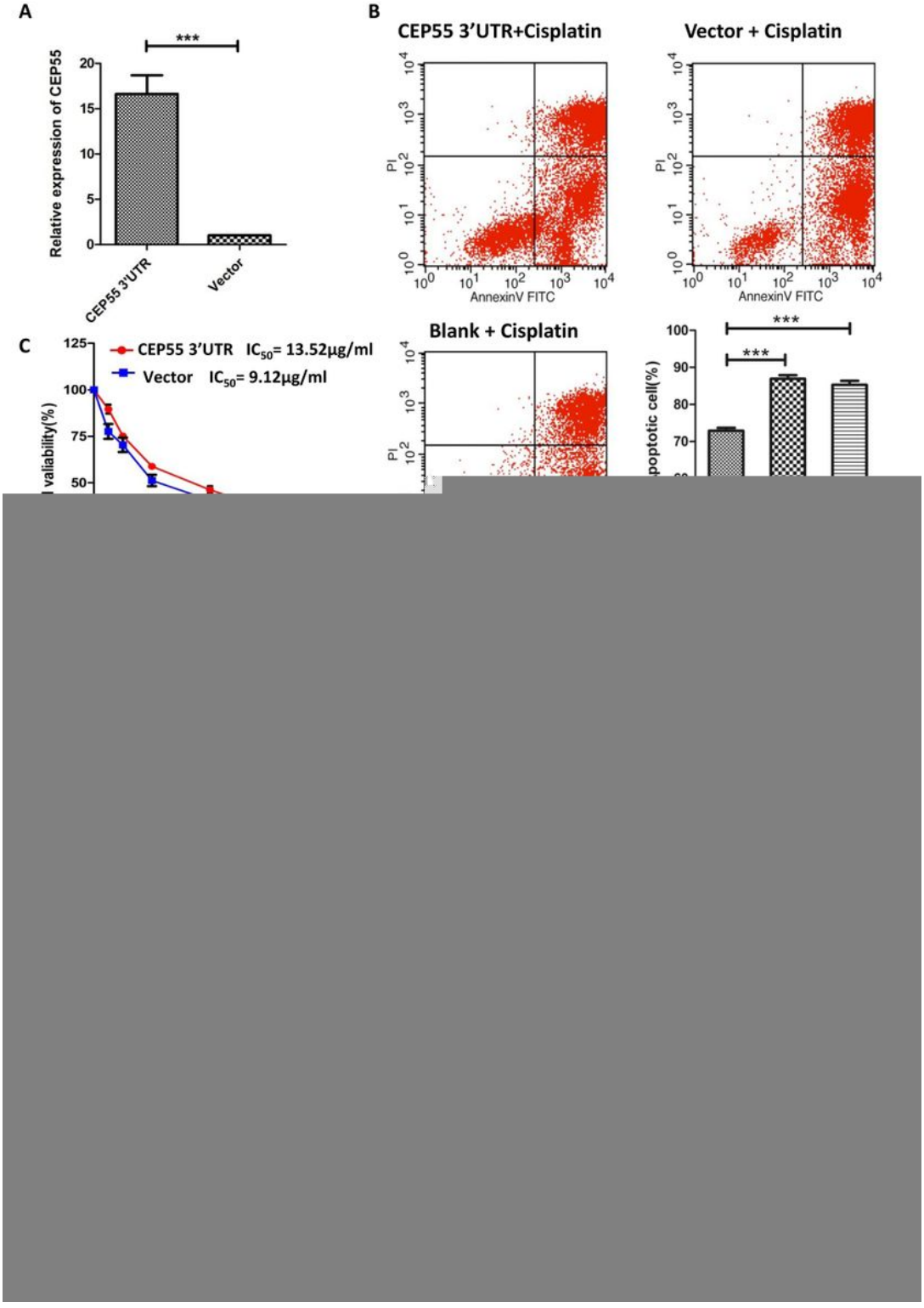

Figure 6

CEP55 3’-UTR reduced the cisplatin sensitivity of BC cells and promoted tumorigenesis in nude mice. (A) Overexpression of CEP55-3’UTR in stably transfected EJ cells. (B) Apoptosis rates of cells stably transfected with CEP55 3’UTR or control vector and treated with cisplatin (8 mg/mL) for 48 h as analyzed by Annexin V/PI staining and flow cytometry. (C) Viabilities of cells stably transfected with CEP55 3’UTR or control vector and treated with cisplatin for 48 h as analyzed by MTT assay. (D and E) Images of tumor xenografts following injection of control EF cells or EJ cells overexpressing CEP55 3’UTR into nude mice. (F and G) Effects of CEP55 3’UTR overexpression on tumor size (F) and weight (G) after 33 days of cisplatin treatment.

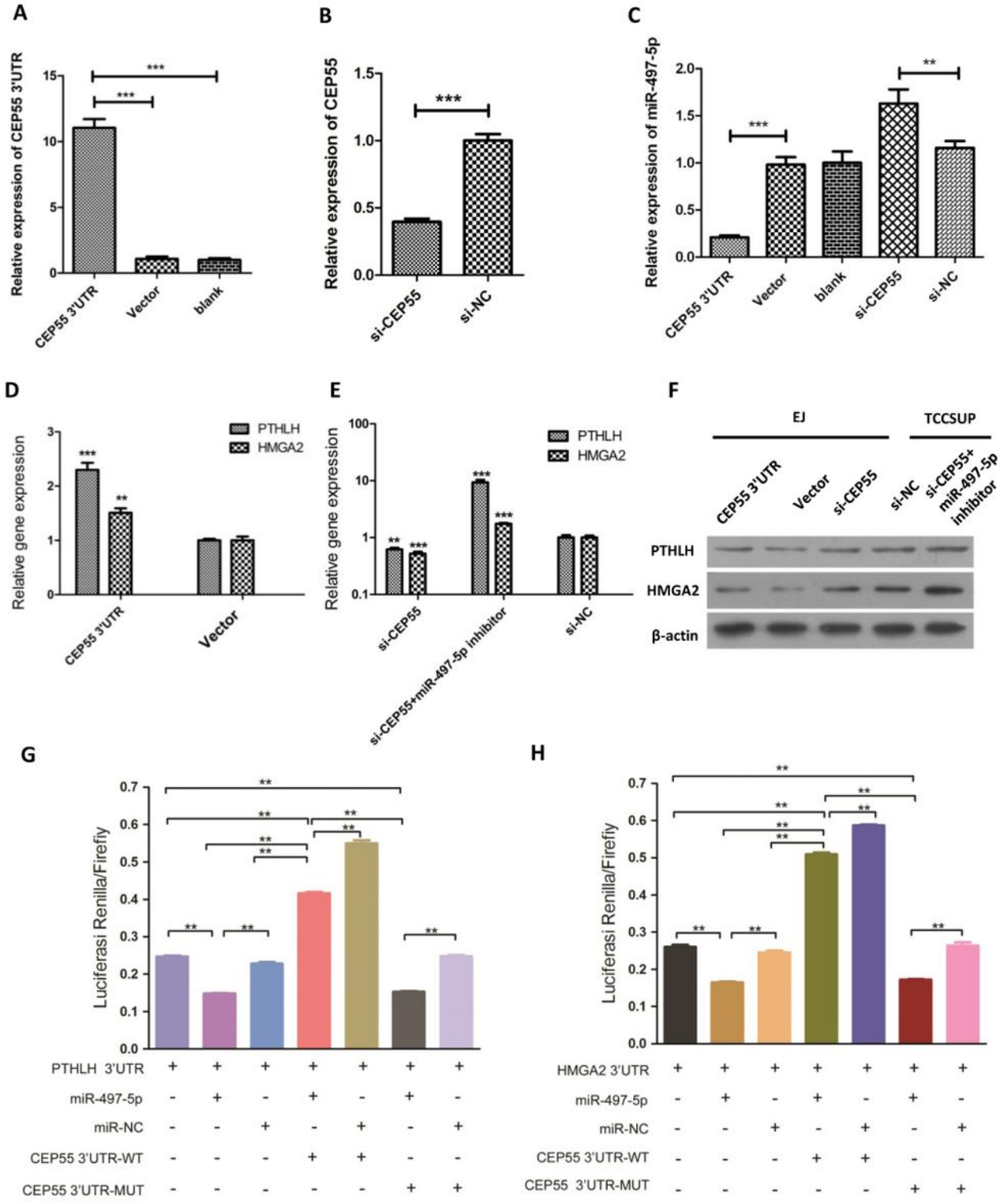

Figure 7

The CEP55 3'UTR functioned as a ceRNA that indirectly regulated PTHLH and HMGA2 expression via miR-497-5p binding. (A and B) EJ cells were transfected with CEP55 3'UTR–pcDNA3.1(+) or empty pcDNA3.1(+) and TCCSUP cells with si-CEP55, si-CEP55 plus miR-497-5p inhibitor, or control siRNA. After 48 h, the efficiency of transfection was confirmed by qRT-PCR. (C-E) Expression levels of PTHLH and HMGA2 mRNAs in transfected cells as measured by qRT-PCR. (F) Expression levels of PTHLH and

HMGA2 proteins in transfected cells as detected by western blot. (G) RLuc-PTHLH 3’-UTR and miR-497-5p constructs were co-transfected into HEK293T cells with plasmids expressing CEP55-3’UTR (CEP55-3’UTR–psiCHECK-2) or with a control vector to verify the ceRNA activity of CEP55-3’UTR. Histogram indicates luciferase activities 48 h after transfection. (H) RLuc-HMGA2 3’-UTR and miR-497-5p constructs were co-transfected into HEK293T cells with plasmids expressing CEP55-3’UTR (CEP55-3’UTR–psiCHECK-2) or with a control vector to verify the ceRNA activity of CEP55-3’UTR. Histogram indicates the luciferase activities measured 48 h after transfection.

Figure 8

The pro-metastasis effect of the CEP55 3’UTR was associated with activation of NF-kB signaling and downregulation of miR-497-5p transcription. (A-B) Western blot analysis of NF-kappaB/p65 in the cytoplasm and nucleus of EJ cells with upregulated or downregulated expression of miR-497-5p or CEP55-3’UTR as indicated. Histone H3 and β-actin were used as gel loading controls for nuclear and cytoplasmic proteins, respectively. (C-D) Immunofluorescence analysis of E-cadherin and vimentin expression after transfection of CEP55-3’UTR–pcDNA3.1(+) or empty pcDNA3.1(+). NF-κB was immunostained red. Nuclei were stained with DAPI (blue). (E) The miR-497-5p promoter sequence upstream of the mature miRNAs sequence. (F-G) Binding sites for NF-κB in the upstream promoter region of miR-497-5p as confirmed by luciferase mutation assay and qRT-PCR.

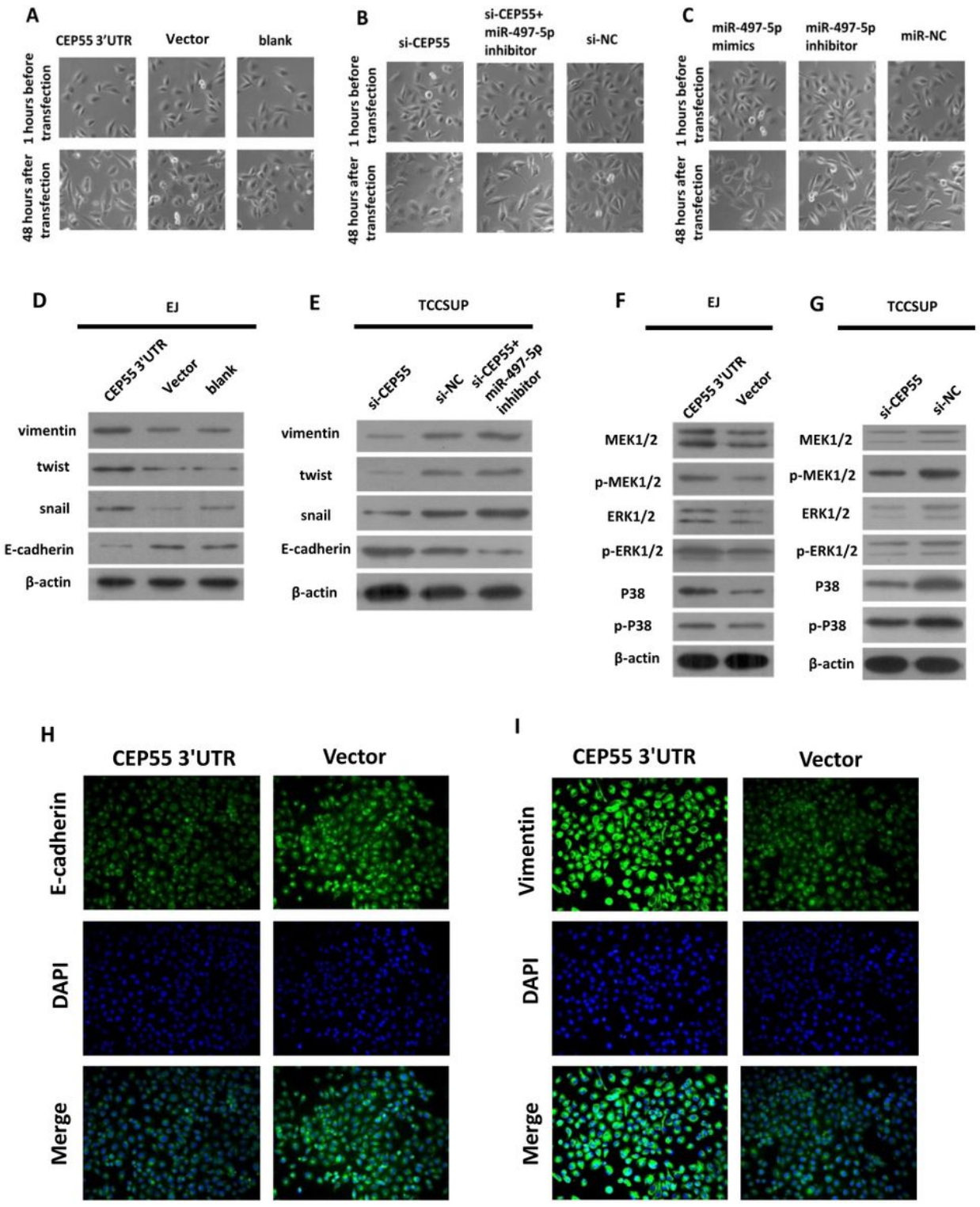

Figure 9

CEP55 3’-UTR induced EMT in EJ and TCCSUP cells by activating p38MAPK and ERK 1/2 pathways. (A-C) Effects of CEP55-3’UTR and miR-497-5p overexpression on EJ cell morphology 48 h after transfection (magnification, ×100). (D-G) EJ cells were transfected with CEP55-3’UTR–pcDNA3.1(+) or empty pcDNA3.1(+) while TCCSUP cells were transfected with si-CEP55, si-CEP55 plus miR-497-5p inhibitor, or control siRNA. After 48 h, protein levels of EMT markers vimentin, twist, snail, and E-cadherin (D and E)

and of the MAPK pathway signaling proteins MEK1/2, p-MEK1/2, ERK1/2, p-ERK1/2, P38, and p-P38, were detected by western blot (F and G). (H-I) Immunofluorescence analysis of E-cadherin and vimentin expression (green) after transfecting CEP55-3'UTR–pcDNA3.1(+) or empty pcDNA3.1(+). Nuclei were stained with DAPI (blue).

Supplementary Files

This is a list of supplementary files associated with this preprint. Click to download.

- CEP55SupplementalTables.docx